

Designing and Optimization of Gear Synchronous Dual-Frequency Induction Heating Power Supply Based on ANSYS

Li Yang

School of Mechatronic Engineering
Xi'an Technological University
Xi'an, China
E-mail: lyiia@sina.com

Lai Hao

Academy of Aerospace Solid Propulsion Technology
AASPT
Xi'an, China
E-mail: 15909200228@163.com

Shang Yaceng

School of Mechatronic Engineering
Xi'an Technological University
Xi'an, China
E-mail: 13279376583@163.com

Su Yichao

School of Mechatronic Engineering
Xi'an Technological University
Xi'an, China
E-mail: 735671048@qq.com

Abstract—Dual-frequency induction heating technology has significant advantages over traditional single-frequency heating for gear quenching. In this paper, the absorption of gear induction heating energy is analyzed theoretically. Based on the simulation of high frequency, medium frequency and dual-frequency magnetic and thermal field with 2-mode 22-tooth gear on ANSYS, it is concluded that the uniformity of the dual-frequency induction heating power supply has obvious advantages in heating. The structure of the dual inverter bridge synchronous dual-frequency induction power supply is studied, the dual inverter bridge synchronous dual-frequency sensor parameters are optimized, and the output variable voltage ratio of 5:1 is determined to achieve the maximum load current inflow to the load.

Keywords—Gear Quenching; Induction Heating; Synchronous Dual Frequency; Variable Pressure Ratio

I. INTRODUCTION

With the development of technology and industry, the demand of energy in recently is increasing, which leads to more and more serious environmental pollution. Therefore, energy conservation, emission reduction and clean environmental pollution have become essential themes in today's society [1]. As the most commonly used components in industrial transmission, gear's heat treatment has become the focus of research. The quenching process is especially important for improving the gear strength. The quenching methods mainly include: traditional surface quenching, carburizing and quenching, and surface nitriding of gear forgings. Compared to the other methods, the cost of traditional quenching is relatively low, besides, it is also the most used method, however, it is difficult to avoid the pollution. Therefore, it is particularly important to find a more efficient and environmentally friendly heat treatment heating technology in industry. In industrial applications, induction heating technology helps to improve the wear resistance and metal fatigue strength of metal workpieces, so that the processed workpiece has the characteristics of small deformation, low brittleness and high hardness [2-3]. Among

them, dual-frequency induction heating technology is mainly used in irregular geometry applications such as gears, sprockets, etc., as well as non-uniform cylindrical workpieces and other single-frequency induction heating technology is limited in the application environment, dual-frequency induction heating has its unique advantages due to the existence of two frequencies, it makes full use of the difference in skin depth at different frequencies, so that the workpiece can be heated uniformly and efficiently [4]. This paper analyzes and optimizes gear frequency sensitivity.

II. PRINCIPLE ANALYSIS OF DUAL FREQUENCY INDUCTION HEATING POWER SUPPLY

A. Theoretical derivation of gear energy absorption

Dual-frequency induction heating refers to heating the current of the tooth tip with a high-frequency component, and heating the root with a medium-frequency component to achieve uniform heating, but the gear of different modulus has an irregular tooth portion., sensitivity to different frequencies is not the same [5]. In the induction heating process, the magnetic field distribution of the irregularly shaped object follows the Maxwell's equations, and in this analysis, the angular portion of the gear can be equivalent to a cylindrical conductor [6]. Ignoring the displacement current, the Ampere loop law is simplified to

$$\nabla \times \vec{H} = \vec{J} \quad (1)$$

In the formula, H means magnetic field strength vector (A/m) and J means current density vector (A/m²)

Assuming that the harmonic variation of the magnetic field strength with time is

$$H(rt) = H(r)e^{-j\omega t} \quad (2)$$

According to Maxwell's differential equation which shows below

$$\begin{cases} \vec{J} = \sigma \vec{E} \\ \vec{B} = \mu \vec{H} \\ \vec{D} = \varepsilon \vec{E} \end{cases} \quad (3)$$

In the formula, μ means magnetic permeability, σ means conductivity and ε means capacitance rate.

We can get,

$$\nabla \times H(r) = \sigma E(r) \quad (4)$$

According to Maxwell's equation

$$\nabla \times \vec{E} = -\frac{\partial B}{\partial t} = -\frac{\partial(\mu \vec{H})}{\partial t} \quad (5)$$

We can get:

$$\nabla \times E(r) = -j\omega\mu H(r) \quad (6)$$

Bringing in

$$\nabla \times \nabla \times H(r) = \nabla \times (\sigma E(r)) = -j\omega\mu\sigma H(r) \quad (7)$$

According to

$$\nabla \times \nabla \times H(r) = \nabla \cdot (\nabla \times H) - \nabla^2 H \quad (8)$$

At the same time, according to the Ampere loop theorem: $\nabla \cdot (\nabla \times H) = 0$. Current diffusion equation is

$$\nabla^2 H = -j\omega\mu\sigma H(r) \quad (9)$$

Taking the column coordinates $H = H(r)e_z$ and $\frac{\partial H}{\partial z} = \frac{\partial H}{\partial \theta} = 0$, we can get

$$\nabla^2 H = \left\{ \frac{1}{r} \frac{\partial}{\partial r} \left(r \frac{\partial}{\partial r} \right) + \frac{1}{r^2} \frac{\partial^2 H}{\partial \theta^2} + \frac{\partial^2 H}{\partial z^2} \right\} e_z = \frac{\partial}{\partial r} \left(r \frac{\partial}{\partial r} \right) e_z = \left(\frac{1}{r} \frac{\partial H}{\partial r} + \frac{\partial^2 H}{\partial r^2} \right) e_z \quad (10)$$

Obtained by (9)-(6), we can get

$$\frac{d^2 H(r)}{dr^2} + \frac{1}{r} \frac{dH}{dr} - j\omega\mu\sigma H(r) = 0 \quad (11)$$

Let $K = j\omega\mu\sigma$, then solve the equation for the magnetic field strength at the cylindrical workpiece r , we can get

$$\frac{d^2 H(r)}{dr^2} + \frac{1}{r} \frac{dH}{dr} - KH(r) = 0 \quad (12)$$

Performing the $\sqrt{K}r$ integration and transforming it into the Bessel equation

$$\frac{d^2 H(r)}{d(\sqrt{K}r)^2} + \frac{1}{\sqrt{K}r} \frac{dH(r)}{d(\sqrt{K}r)} - H(r) = 0 \quad (13)$$

The skin depth expression is as follows

$$\delta = \sqrt{\frac{2\rho}{\omega\mu}} = \sqrt{\frac{\rho}{\pi f \mu}} \quad (14)$$

Among them, ρ means resistivity and the conductivity of material defined by $\gamma = 1/\rho$

$$\text{Assuming } m = r\sqrt{\omega\mu\sigma}, \text{ then } m = \frac{\sqrt{2}r}{\delta}, \quad m_2 = \frac{\sqrt{2}R_0}{\delta}$$

Cylindrical workpiece current density is

$$J = \frac{\sqrt{2}jH_0}{\delta} \frac{I_1(\sqrt{j}m)}{I_0(\sqrt{j}m_2)} \quad (15)$$

Where I_0, I_1 are zero order and first order first class Bessel functions

$$\begin{cases} I_0(\sqrt{j}m) = ber m + jber m \\ I_1(\sqrt{j}m) = ber' m + jber' m \end{cases} \quad (16)$$

When $m_2 \leq 2$, $ber^2 m + jber^2 m = 1$

$$ber'^2 m + jber'^2 m = \frac{m^2}{4}$$

$$J = \frac{H_0}{\delta^2} r \quad (17)$$

Eddy current volume heating power is as below

$$q_v = \frac{J^2}{\sigma} \quad (18)$$

Taking a micro-element with a thickness of dr and a height of $z=1$ on the r -axis, the volume of which is $dv = 2\pi r dr$, the heat generated by the volume per unit time is

$$dq_v = 2\pi \frac{H_0^2 r^3}{\sigma \delta^4} dr \quad (19)$$

Heat absorbed per unit volume is as below. Bringing it into formula (14) and scoring, we can get

$$Q_0 = \frac{\pi^2}{2} H_0^2 \sigma \mu^2 f^2 m^2 z^2 \quad (20)$$

The formula for absorbing energy per unit volume gear is $R_0 = \frac{mz}{2}$

$$Q_0 = \frac{\pi^2}{2} H_0^2 \sigma \mu^2 f^2 \frac{m^2 z^2}{4} = \frac{\pi^2}{8} H_0^2 \sigma \mu^2 f^2 m^2 z^2 \quad (21)$$

It is not difficult to see that the absorbed heat is proportional to the square of the modulus, Q_0 is determined by the heating time and temperature, and the heating time is t .

$$Q_0 = \frac{4Pt}{B\pi m^2 z^2} = \frac{\pi^2}{8} H_0^2 \sigma \mu^2 f^2 m^2 z^2 \quad (22)$$

At the same time we can draw

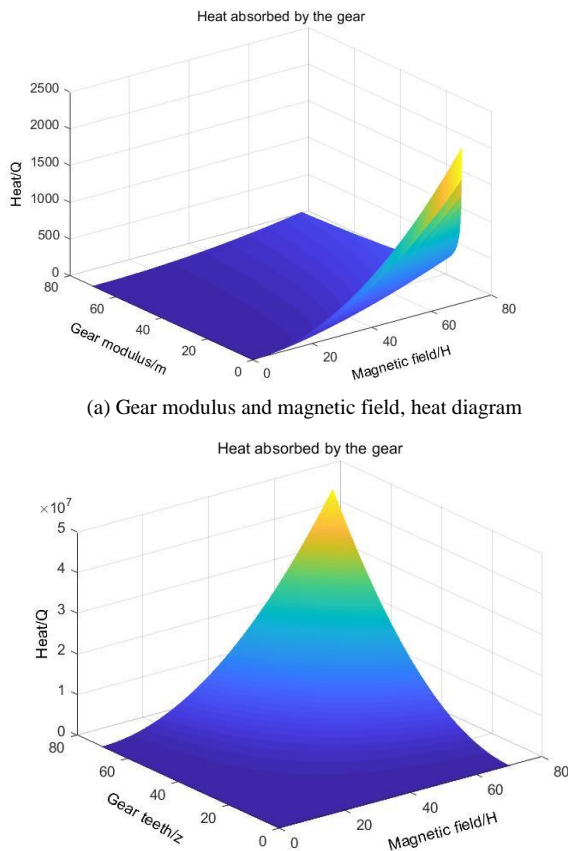
$$f = \sqrt{\frac{32Pt}{\mu^2 H_0^2 \pi^3 m^4 z^4}} = \frac{4\sqrt{2Pt}}{\mu H_0 m^2 z^2 \sqrt{B\sigma\pi}} \quad (23)$$

It is easy to see that f is inversely proportional to m^2 . According to the empirical formula of Soviet scholars

$$f = \frac{600}{m^2} (\text{KHz})$$

$$Q = Q_0 t = \frac{\pi^2}{2} H_0^2 \sigma \mu^2 \left(\frac{600000}{m^2}\right)^2 \frac{m^2 z^2}{4} t = \frac{\pi^2}{8} H_0^2 \sigma \mu^2 \left(\frac{600000}{m^2}\right)^2 m^2 z^2 t \quad (24)$$

According to the derivation formula, it is not difficult to see that the energy absorption of the gear is inversely proportional to the square of the modulus and the square of the number of teeth. According to the three parameters of the gear modulus, the number of teeth and the tooth width, the corresponding energy can be obtained according to the empirical formula. Figure 1 shows the gear modulus and the relationship between the number of teeth and the magnetic field and heat.



(a) Gear modulus and magnetic field, heat diagram

(b) Gear tooth number and magnetic field, heat relationship diagram

Figure 1. Figure of gear modulus and magnetic field, heat

B. Dual frequency heating power principle

The synchronous dual-frequency induction heating power supply means that the induction coil is simultaneously provided with an intermediate frequency current and a high frequency current, that is, a current of an intermediate frequency envelope high frequency is generated on the

induction coil. The synchronous dual-frequency induction heating power supply can be divided into a single inverter bridge synchronous dual-frequency induction heating power supply and a dual inverter bridge synchronous dual-frequency induction heating power supply [7-10]. As is shown in Figure 2 below, the topology corresponds to a set of high frequency induction heating power supply and a set of intermediate frequency induction heating power supply, and two sets of induction heating power sources work together to one output. When two sets of induction heating power sources are simultaneously activated, a resonant current superposed by a high-frequency resonant current and an intermediate frequency resonant current can be obtained on the induction coil, thereby achieving the purpose of synchronous dual-frequency output, and uniformly quenching the gears [11-13].

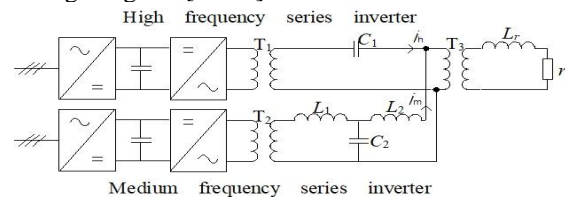


Figure 2. Synchronous dual-frequency quenching topology

III. SIMULATION ANALYSIS OF TEMPERATURE FIELD BASED ON ANSYS DUAL FREQUENCY POWER SUPPLY

A. Simulation power selection

The power density of the induction heating device is mainly determined by the surface area of the quenched workpiece and the quenching technique [14]. If the size of the quenched workpiece is small, the depth of the hardened layer required is shallow, and the current frequency on the inductor is small, the power density of the induction heating device should be relatively large [15]. It is determined through investigation that in the dual-frequency induction heating power supply, when the medium frequency induction heating power source is used for heating, the power density usually is $0.8 - 2 \text{ kW/cm}^2$; When heating with a high frequency induction heating power supply, the power density usually is $0.6 - 2.5 \text{ kW/cm}^2$. In this paper, the 2-mode 22-toothed gear is taken as the research object. The structure is solid gear, and the volume of the tooth root is 2.4 times the volume of the irregular shape. In order to ensure the uniformity of heating, the ratio of the intermediate frequency and the high frequency power is 2 : 1. The total power of the dual-frequency induction heating power supply to be designed in this subject is 75kW, so the medium frequency power designed in this paper is 50kW, and the high frequency power is 25kW.

B. Simulation frequency selection

The depth of the hardened layer of the gear is related to the application of the gear. For different applications, the depth of the hardened layer required will vary. This paper chooses to use 2 modes and 22 teeth as the research object. The depth of the hardened layer is related to the penetration depth of the current, moreover, when the relationship

between the depth of the hardened layer and the penetration depth is $\delta = 2D_s$, the induction heating device can obtain high thermal efficiency, thereby achieving the effects of good energy saving effect, short heating time, and high work efficiency. And in the case of eliminating the self-attenuation of the spectrum, the sensitive frequency of the irregular portion of the tooth tip is 13kHz. Therefore, the high frequency heating frequency is 80kHz. Similarly, the intermediate frequency heating frequency is 13kHz.

C. Simulation analysis based on maxwell electromagnetic field

The main gear used in this paper is a spur gear with 22 teeth and a material of 45# steel. The inductor has a coil inner diameter of 50 mm, an outer diameter of 70 mm, a wall thickness of 2 mm, and a material of copper. Firstly, pulling out the standard 2-mode 22-tooth gear in the Solidworks standard parts library, and then building the sensor model, assembling the two and importing them into Maxwell. The simulation model is shown in Figure 3.

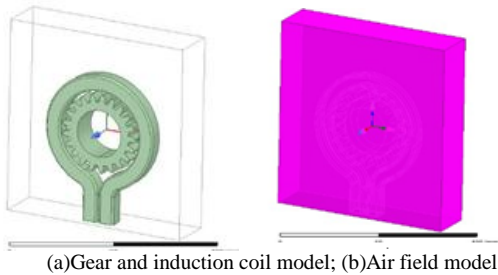


Figure 3. Establishment of coupled field simulation model

Figure 4 shows the magnetic induction intensity distribution on the gears solved in Maxwell. Due to the skin effect, the induced eddy current field is mainly concentrated on the gear surface. Subsequently, the simulation results were imported into ANSYS for transient thermal field simulation.

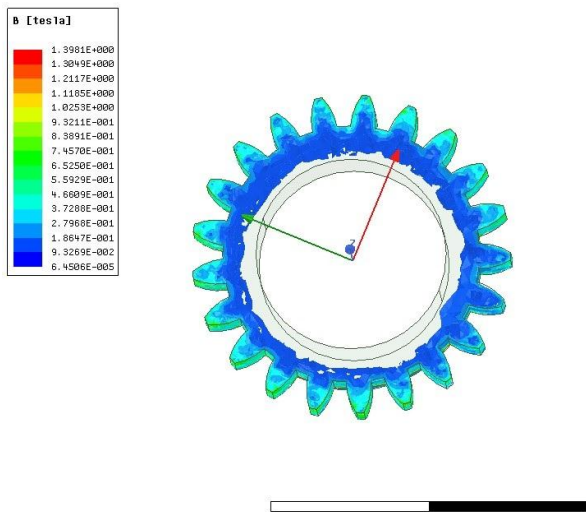


Figure 4. Gear magnetic induction distribution map

D. Thermal coupling simulation analysis based on workbench

In this section, the large-scale general software ANSYS is used for simulation analysis. The results of the electromagnetic field analysis in Maxwell are introduced into ANSYS for thermal field analysis by sequential coupling method, and the eddy current obtained by electromagnetic field analysis is used for transient thermal analysis. An electromagnetic-thermal coupled field simulation model for gear quenching is established. In this process, it is necessary to find the time point at which the temperature gradient is maximum, and the node temperature at this time point is applied as a load to the gear for analysis. After the model is imported, the mesh is divided. The mesh is divided as shown in Figure 5. Since the accuracy of the meshing has a large impact on the overall analysis, in this analysis, the gears are more densely divided. In the induction heating process, heat is mainly concentrated on the surface of the gear, which is beneficial to the accuracy of the calculation results. In the thermal simulation process, it is assumed that the current given by the inductor is a uniform current, so that the sensor is sparsely divided, which reduces the amount of calculation, thereby greatly saving computing resources. Subsequently, a setting of boundary conditions and mapping excitations is performed, which is the initial temperature of the entire model, where it is set to room temperature 25 °C.

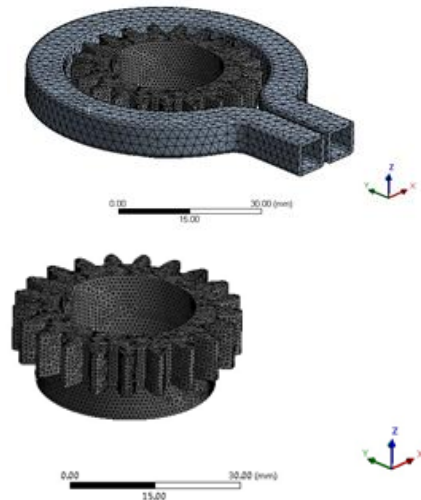
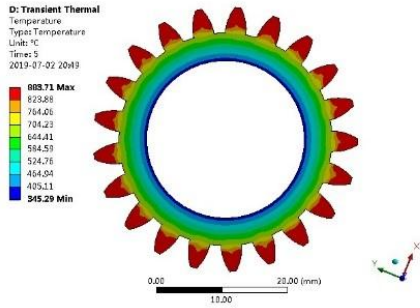


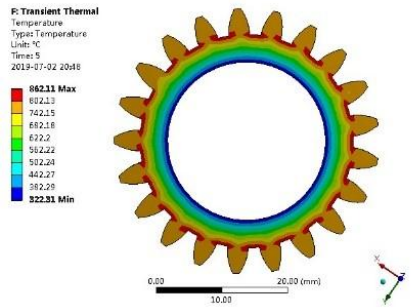
Figure 5. Gear and sensor meshing

According to the operation, the following results are obtained. Under the action of a single high frequency, the maximum temperature of the gear reaches 883.70 °C. The root temperature is about 760.06 °C, and the root and tip of the tooth are not uniformly heated. Under the action of a single intermediate frequency, the maximum temperature of the gear reaches about 862.11 °C, mainly distributed in the root portion, and the tip temperature is about 714.25 °C. Although both of them reaching the quenching temperature, the heat is obviously uneven. Under the action of dual-frequency heating, the temperature of the root and the tip of the tooth reached about 862.40 °C, which satisfies the quenching process requirements of the gear. In terms of heat

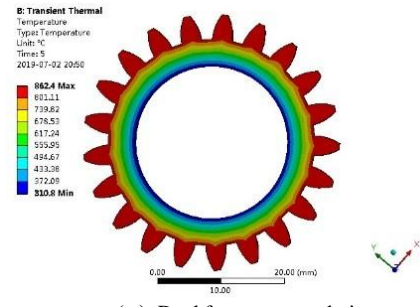
uniformity, the advantages of dual frequency heating are obvious.



(a) Single high frequency rendering



(b) Single intermediate frequency rendering



(c) Dual frequency rendering

Figure 6. Thermal field simulation analysis

IV. HARDWARE OPTIMIZATION DESIGN BASED ON PSIM

A. Variable ratio quantitative model establishment

According to the Ansys simulation results, and in the case of eliminating the self-attenuation of the spectrum, the sensitive frequency of the irregular portion of the tooth tip is 13 kHz. Therefore, the high frequency heating frequency is 80 kHz, and the intermediate frequency heating frequency is 13 kHz.

Since the two are heated for different parts of the gear, the equivalent load is different, and the equivalent load $r=0.01W$ (high frequency), $r=0.0032W$ (intermediate frequency) are selected. The simulation model is established, and T3 is used as the output transformer, which directly determines the load of the hardware parameters of the circuit, so the simulation is performed with the output transformer.

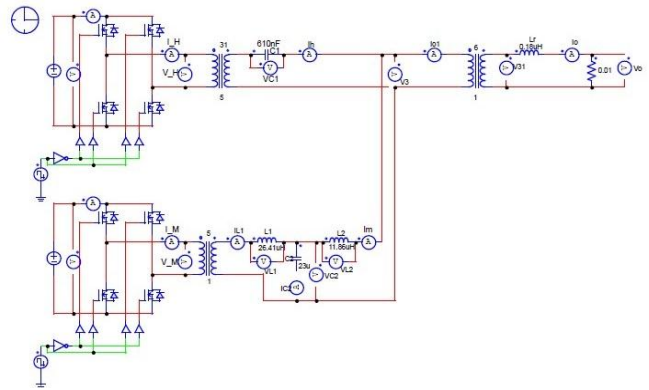


Figure 7. Circuit model construction (taking 6:1 as an example)

TABLE I. GROUP 1 4:1 RATIO MODEL PARAMETERS

Component name	T1	T2	T3(secondary side)	C1	C2	L1	L2
parameter	19:2	33:5	4:1	1.37uF	49.5uF	13.25uH	5.27uH
I _{pk} /A	108.6	109.5	2658(HF)+4728(MF)	1031.7	369(HF)+761(MF)	722.5	368(HF)+1164(MF)
V _{pk} /V	514	514	314(HF)+55.7(MF)	1201	602	679	1267(HF)+385(MF)

TABLE II. GROUP 2 5:1 RATIO MODEL PARAMETERS

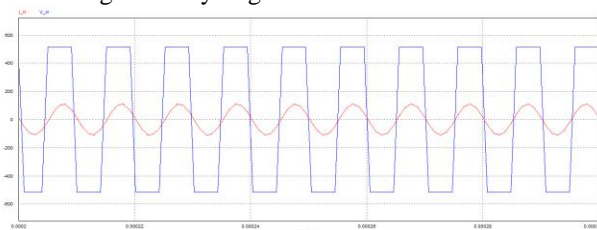
Component name	T1	T2	T3(secondary side)	C1	C2	L1	L2
parameter	15:2	5:1	5:1	880nF	31uF	21.9uH	8.23uH
I _{pk} /A	110.6	108.9	2673(HF)+4716(MF)	829.5	298(HF)+1463(MF)	544.5	296(HF)+929(MF)
V _{pk} /V	514	514	315(HF)+55.5(MF)	1507	750	851	1590(HF)+480(MF)

TABLE III. GROUP 3 6:1 RATIO MODEL PARAMETERS

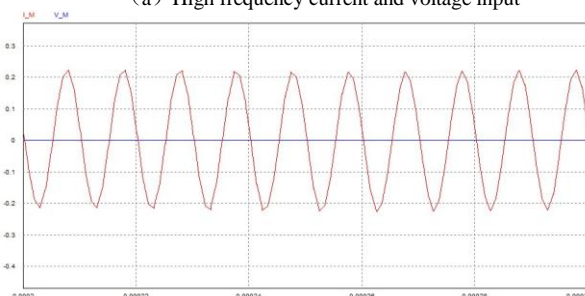
Component name	T1	T2	T3(secondary side)	C1	C2	L1	L2
parameter	31:5	5:1	6:1	610nF	23uF	26.41uH	11.86uH
I _{pk} /A	112.7	106.5	2702(HF)+4667(MF)	698.7	250(HF)+1291(MF)	532.5	249(HF)+766(MF)
V _{pk} /V	514	514	319(HF)+54.9(MF)	1830	890	986	1930(HF)+569(MF)

B. Simulation result analysis

As is shown in the figure below, Figure 8 (a), (b) show the input current and voltage waveforms of high-frequency and medium frequency at the 5:1 ratio respectively. As can be seen from the figure the peak of the high-frequency power supply current is approximately 1031.7A, the peak of the high-frequency current flowing into the intermediate-frequency branch is 368A and the peak value of the high-frequency current flowing into the load is 664.5A. The peak value of the output current of the intermediate-frequency power supply is approximately 1164A. The peak value of the intermediate frequency current flowing into the high frequency branch is 19.2A, and the peak value of the intermediate frequency current flowing into the load is 1182A. At this point, the peak value of the inflow load current is significantly larger than the other ratios.



(a) High frequency current and voltage input



(b) Intermediate frequency current and voltage input

Figure 8. High frequency intermediate frequency input current and voltage waveform

V. CONCLUSION

Firstly, based on the loop amperage law, the energy absorption of the induction heating and the geometrical parameters of the gear are analyzed. It is found that the energy absorption of the gear is inversely proportional to the square of the modulus and proportional to the square of the number of teeth. Then the circuit topology of the synchronous dual-frequency induction heating power supply is analyzed, and the thermal field analysis is carried out based on Ansys with 2 mode 22 tooth gears. It is concluded that the dual frequency induction heating power supply has obvious advantages in heating uniformity. After that, based on PSmin to build a circuit simulation model and simulate the output transformer, the output transformer input load

current of 5:1 is the largest. Synchronous dual-frequency induction heating technology has higher energy efficiency and more uniform quenching temperature than conventional methods.

ACKNOWLEDGMENT

I sincerely thank my teachers and school as well as POLARIS ETek Co., Ltd. This is my teacher's help and supported by the Science and Technology Innovation Project of Shaanxi Province (No. 2015KTZDGY-02-01).

REFERENCES

- [1] Wang Liping. Research on induction heating power supply for heat-treating of gear[D].Xi'an:Xi'an University of Technology, 2016.
- [2] Hou Peng.Research of dual-frequency induction heating power supply [D].Chengdu : University of Electronic Science and Technology of China, 2015.
- [3] Chen Zhuogunag. Research of a new type of dual-frequency induction heating circuit [D].Xi'an: Xi'an University of Technology, 2015.
- [4] He Ting. Research of simultaneous dual-frequency induction heating power supply based on single inverter [D].Beijing:Tsinghua University, 2013.
- [5] Yang Yameng.Study on synchronous dual-frequency induction heating power supply [D].He Nan : Zheng Zhou University, 2017.
- [6] Sun Dan. Frequency sensitivity analysis and research of irregular shape objects in induction heating [D].Xi'an: Xi'an University of Technology,2015.
- [7] Wang Zhiming. The new technology of gear's simultaneous dual frequency induction hardening[J].Machanical Drive , 2012,36(11):108-110.
- [8] Zhang Bai, Ma baihui. Gear induction true contour hardening with SDF[J].Heat Treatment of Metals, 2010,35(6):127-129.
- [9] Tian Di. Based on the principle of dual-frequency waveform synthesis induction heating power supply[D]. Xi'an: Xi'an University of Technology, 2014.
- [10] Shan Yue.Research on the double frequency output of the induction heating power supply[D]. Xi'an: Xi'an University of Technology,2013.
- [11] Dede Garcia-Santamaria E J, Esteve Gomez V, Jordan Martinez J, et al. Inductive heating apparatus comprising a resonant circuit with simultaneous dual frequency current output and a single inverter circuit with silicon carbide: EP, EP2 14855 1 [P]. 2010.
- [12] Esteve V, Jordan J, Sanchis-Kilders E, et al. Comparative Study of a Single Inverter Bridge for Dual-Frequency Induction Heating Using Si and SiC MOSFETs[J]. Industrial Electronics IEEE Transactions on, 2015, 62(3):1440-1450.
- [13] Esteve V, Jordan J, Sanchis-Kilders E, et al. Improving the Reliability of Series Resonant Inverters for Induction Heating Applications[J]. IEEE Transactions on Industrial Electronics, 2013, 61(5):2564-2572.
- [14] Wang Jin.Rasearch on dual frequency induction heating power supply for gear heat treatment [D].Xi'an: Xi'an University of Technology,2018.
- [15] Shi Peigang.Study on dual frequency induction heating power supply used for normalizing of rail welding [D].Xi'an: Xi'an University of Technology,2017.